



BORDER COLLISION BIFURCATIONS IN 1D PWL MAP WITH ONE DISCONTINUITY AND NEGATIVE JUMP. USE OF THE FIRST RETURN MAP

LAURA GARDINI* and FABIO TRAMONTANA†
*Department of Economics and Quantitative Methods,
University of Urbino, Italy*
**laura.gardini@uniurb.it*
†*f.tramontana@univpm.it*

Received January 8, 2010

The aim of this work is to study discontinuous one-dimensional maps in the case of slopes and offsets having opposite signs. Such models represent the dynamics of applied systems in several disciplines. We analyze in particular attracting cycles, their border collision bifurcations and the properties of the periodicity regions in the parameter space. The peculiarity of this family is that we can make use of the technical instrument of the first return map. With this, we can rigorously prove properties which were known numerically, as well as prove new ones, giving a complete characterization of the overlapping periodicity regions.

Keywords: Discontinuous piecewise linear 1D map; increasing–decreasing map; border collision bifurcations; increment bifurcation structure.

1. Introduction

It is well-known that several models are described by piecewise smooth dynamical systems (PWS for short). The essential feature in PWS systems (continuous or discontinuous) is the presence of a change of definition in the functions defining the map under study, when a suitable border is met or crossed. This leads to the existence of *border collision bifurcations* (BCB henceforth). The first works on this subject date back to [Leonov, 1959, 1962] and [Mira, 1978, 1987], and have been studied more recently by [Nusse & Yorke, 1992, 1995; Maistrenko *et al.*, 1993; Maistrenko *et al.*, 1995; Maistrenko *et al.*, 1998]. In the last few years, many papers have been published which deal with PWS systems, due to their wide use in the applied context. We recall, for example, the books [Banerjee & Verghese, 2001; Zhusubaliyev & Mosekilde, 2003; di Bernardo *et al.*, 2008]. Besides the works cited above, piecewise smooth systems are applied in power electronic circuits [Halse *et al.*, 2003; Banerjee *et al.*, 2000],

impacting systems ([Nusse *et al.*, 1994; Ing *et al.*, 2008; Sharan & Banerjee, 2008] to cite a few), piecewise smooth nonlinear oscillators [Pavlovskaja *et al.*, 2004; Pavlovskaja & Wiercigroch, 2007] and in many other applications [Banerjee & Grebogi, 1999; di Bernardo *et al.*, 1999; Sushko *et al.*, 2005, 2006].

The observed dynamics (and BCB properties) differ depending on continuous or discontinuous models. Here, we are interested in discontinuous ones, which have also been studied in some particular cases in recent works (see, for example, [Kollar *et al.*, 2004; Avrutin & Schanz, 2005, 2006, 2008; Avrutin *et al.*, 2006]). The characteristic features are the particular bifurcation structures which follow the so-called *period adding* and *period increment* scheme. The results, however, are particularly important with respect to the bifurcations occurring to the chaotic intervals as studied in [Avrutin *et al.*, 2007, 2008a, 2008b, 2009; Avrutin *et al.*, 2010c].

In this paper, we consider the one-dimensional canonic form suitable for studying the bifurcations occurring in discontinuous one-dimensional maps already introduced by Leonov, and considered in [Gardini *et al.*, 2010] and [Avrutin *et al.*, 2010b], with particular restrictions on the parameters, as the analysis of the bifurcations occurring in all the possible cases is still far from complete. Here we contribute to the study of another particular situation in the parameter space of this one-dimensional map in canonic form, related to the cases of slopes and offsets having opposite signs. We are interested in the bifurcations occurring in the periodicity regions of attracting cycles. The occurrence of the period increment scheme is well-known, but the properties related to this bifurcation structure have not been fully described up to now. This is the object of the present work. Let us consider the one-dimensional piecewise linear map in canonical form:

$$x' = f(x) = \begin{cases} f_L(x) = a_L x + \mu_L, & \text{if } x < 0 \\ f_R(x) = a_R x + \mu_R, & \text{if } x > 0 \end{cases} \quad (1)$$

in which the slopes and the offsets have opposite signs. That is, we consider the parameter space with:

$$a_R a_L < 0, \quad \mu_L \mu_R < 0 \quad (2)$$

We recall that (as already remarked by Leonov) although by rescaling the state variable one parameter may be set to a constant value, we keep the notation in full because this simplifies the expressions in the formulas of the BCB curves.

In order to study the dynamic behaviors of $f(x)$, the considered restriction in the parameters, given in (2), allows for a suitable use of the technique of the *first return map*. With the first return map we have found a simplified expression for some BCB curves of the stable cycles, and particular properties associated with the points of intersection of the BCB curves and the flip bifurcation curves. In particular, we shall recover and rigorously prove the properties of the parameter regions which are associated with the *period increment* behaviors. As is well-known, in that region *at most two attracting cycles can coexist*. Moreover, we shall see that, as long as the map is invertible in the invariant absorbing interval, *when only one stable cycle exists, then at most one unstable cycle can coexist (and clearly no chaotic set)*. When the map is noninvertible in the invariant absorbing interval, chaos may occur in

attracting cyclic chaotic intervals, and is robust (following [Banerjee *et al.*, 1998]), as persistent under parameter perturbations, *or chaos may occur only in a chaotic repeller*. In the parameter region associated with chaotic dynamics, *regions (or islands) of stable cycles can exist but not a pair of attractors*.

The work is organized as follows. Some general properties are recalled in Sec. 2, while in Sec. 3, we shall consider the particular case $a_L a_R = -1$, showing that we can have coexistent cycles also with four different periods. The particular case $a_L a_R = 0$ is considered in Sec. 4, showing that only one attracting cycle can exist. The analysis of the generic cases in the parameters (2) is performed in Sec. 5. Here in different subsections, by using the first return map, we shall prove peculiar properties of the overlapping (in pair) stability regions, also giving a simplified expression of the BCB curves already determined in other works ([Gardini *et al.*, 2010; Avrutin *et al.*, 2010b], and references therein), as well as the proof of the properties listed above.

2. General Properties

Let us consider the map in the generic form given in (1), assuming $a_L > 0$ and $a_R < 0$, when the shape of the function is increasing for $x < 0$, let us say on the L side, and decreasing for $x > 0$, let us say on the R side. Then the dynamics associated with the signs $\mu_L < 0$ and $\mu_R > 0$ are very simple, because a fixed point always exists on the R side, $Q^* = \mu_R / (1 - a_R) > 0$ (stable or unstable, depending on the slope a_R) while on the L side $P^* = \mu_L / (1 - a_L) < 0$ exists only if it is stable, and in both cases the related dynamics are quickly seen.

The interesting cases are associated with $\mu_L > 0$ and $\mu_R < 0$, when the shape of the function is as shown in Fig. 1(a). Then inverting the signs of the two slopes the reasoning is the same, and the maps are topologically conjugated. In fact, the map in Fig. 1(b) is conjugated with that in Fig. 1(a) via the following symmetry property of $f(x)$:

$$\begin{aligned} f(x, a_R, a_L, \mu_L, \mu_R) \\ = -f(-x, a_L, a_R, -\mu_R, -\mu_L) \end{aligned} \quad (3)$$

It follows that we can restrict our analysis to the case $a_L > 0$ and $a_R < 0$ with $\mu_L > 0$ and $\mu_R < 0$ (whose shape for $a_L > 1$ is shown in Fig. 1(a)).

It is clear that considering a point on the R side, in one iteration it is mapped to the other (L) side, from where either the trajectory is divergent or the map f_L is applied until the iterated point enters the

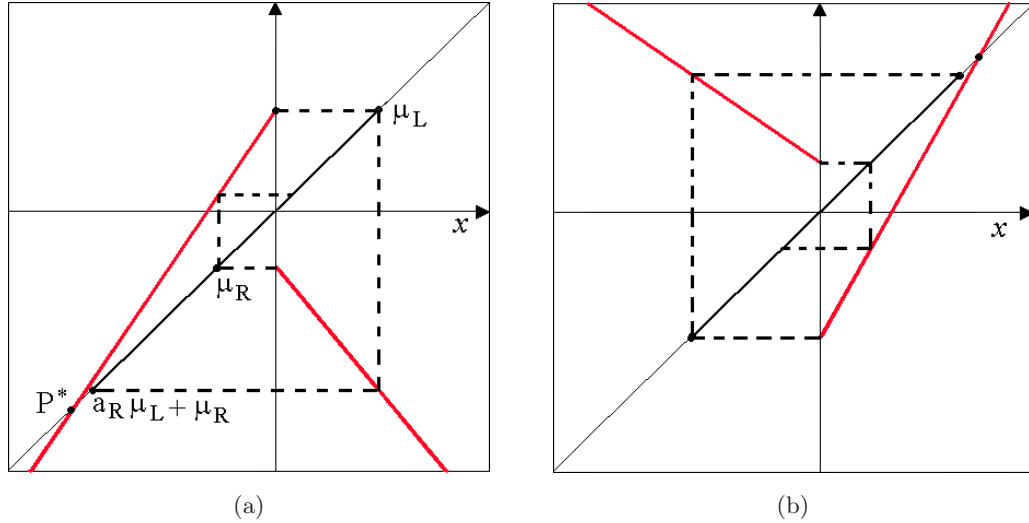


Fig. 1. Qualitative shape of the map considered in this work.

positive side again. Under our assumptions there is no fixed point on the R side, and as long as $0 < a_L \leq 1$ there is also no fixed point on the L side. In this case ($0 < a_L \leq 1$) all the trajectories of the map will enter in the invariant absorbing interval

$$I = [a_R\mu_L + \mu_R, \mu_L] \tag{4}$$

in a finite number of iterations (and its basin of attraction will be the entire real line). The fixed point P^* on the L side exists when it is unstable, for $a_L > 1$, and then all the points below P^* have a trajectory which is divergent to $-\infty$, while the negative points above P^* (i.e. for $\mu_L/(1 - a_L) < x < 0$) have a trajectory which enters the absorbing interval I , as long as the following inequality holds:

$$P^* = \frac{\mu_L}{1 - a_L} < a_R\mu_L + \mu_R \tag{5}$$

which guarantees that the invariant interval I has no contact with its basin of attraction, so that it is absorbing. In this case, the basin of divergent trajectories is given by

$$\mathcal{B}(\infty) =]-\infty, P^*[\cup]P_{-1}^*, +\infty[\tag{6}$$

where P_{-1}^* is the preimage of the fixed point on the R side, given by the solution of the equation $P^* = a_Rx + \mu_R$, that is:

$$P_{-1}^* = \frac{\mu_L - \mu_R + \mu_R a_L}{a_R(1 - a_L)} \tag{7}$$

Here the denominators in P^* and P_{-1}^* are assumed different from zero, as the particular cases with

$a_L = 1$ or with $a_R = 0$ are considered in separate sections. Clearly the complementary set of $\mathcal{B}(\infty)$ (given in (6)) in the real line, gives us the basin of attraction of the absorbing interval I :

$$\mathcal{B}(I) =]P^*, P_{-1}^*[= \left] \frac{\mu_L}{1 - a_L}, \frac{\mu_L - \mu_R + \mu_R a_L}{a_R(1 - a_L)} \right[\tag{8}$$

as we exclude the frontier, which is itself an invariant set. As remarked above, the equality in (5) denotes a bifurcation. When the condition

$$\chi_{\text{div}}: \frac{\mu_L}{1 - a_L} = a_R\mu_L + \mu_R \tag{9}$$

holds, a contact of the invariant interval I with its basin of attraction occurs, and this denotes a “final bifurcation” because it is followed by a dynamic made up of almost all divergent trajectories when $P^* > a_R\mu_L + \mu_R$.

Thus we are interested in parameters which satisfy the condition in (5) for which we can restrict the study of the map inside the absorbing interval I . Moreover, as noticed above, we can fix an initial condition on the R side, $0 < x < \mu_L$. That is, let $J_R = [0, \mu_L] = I \cap \{x \geq 0\}$, then we can simply construct the “first return map F_R ” in J_R , given by:

$$F_R: x \in J_R \rightarrow f^m(x) \in J_R, \quad J_R = [0, \mu_L] \tag{10}$$

where m is the first integer for which $f^m(x) \in J_R$. This map F_R describes all the BCB occurring to the map f in I . We remark that in general there is not a unique integer m for all the points of J_R . The analysis of the particular cases performed in the

next Secs. 3 and 4 provides examples of the power of the investigation of the dynamics using the first return map F_R .

3. Particular Case $a_L = 1$ and $a_R = -1$

In this particular case, the map is only a function of the offsets $\mu_R (< 0)$ and $\mu_L (> 0)$:

$$x' = f(x) = \begin{cases} f_L(x) = x + \mu_L, & \text{if } x < 0 \\ f_R(x) = -x + \mu_R, & \text{if } x > 0 \end{cases} \quad (11)$$

It is easy to see that we cannot have fixed points of f , and the dynamics are trapped in the invariant absorbing interval

$$I = [-\mu_L + \mu_R, \mu_L] \quad (12)$$

as any other point is mapped into I in a finite number of steps. Depending on the parameters, it is possible to have stable (but not attracting) periodic orbits of any period, as shown in the bifurcation diagram in Fig. 2, as a function of μ_L . Such periodic orbits are not attracting because of the particular case, and all the eigenvalues of the existing cycles are either $+1$ or -1 . We shall see that any point of the absorbing interval I is a periodic point, i.e. it belongs to some cycle of a given period, and as a consequence, any point outside I is preperiodic (which means that it is mapped into a periodic point in a finite number of steps).

Clearly the period of the cycle depends on the values of parameters μ_R and μ_L . Moreover, at any fixed value of the parameters there is no unique period, but two and even four different periods.

To see this and to describe the bifurcations leading to the changes in the periods of the cycles we make use of the first return map F_R .

We know that the discontinuity point behaves as a critical point, in determining the BCB (as a collision occurs due to a merging with the discontinuity point). A particular role is also played by the trajectories associated with the two values in the discontinuity point: $f_R(0) = \mu_R$ and $f_L(0) = \mu_L$. Here, we have a unique critical trajectory, as it can be immediately seen that

$$\begin{aligned} f_R(0) = \mu_R &= f_L \circ f_R(\mu_L) \\ &= f_L \circ f_R \circ f_L(0) \end{aligned} \quad (13)$$

and a particular integer determines the first return of the critical orbit in the interval J_R for the return map F_R . In fact, let $d = F_R(\mu_L)$, then this point d separates the interval of definition of the return map ($J_R = [0, \mu_L]$) in two different subintervals, having different properties. Let $k \geq 1$ be the integer defining the number of iterations (with f_L) to apply to μ_R in order to get a positive point, say d , that is:

$$d = f_L^k(\mu_R) = f_L^{k+1} \circ f_R(\mu_L) > 0 \quad (14)$$

and in explicit form:

$$d = \mu_R + k\mu_L \quad (15)$$

We shall see that when the critical point d is positive, it separates the interval J_R into two pieces:

$$J_R = C_l(J' \cup J''), \quad J' =]0, d[, \quad J'' =]d, \mu_L[\quad (16)$$

(where C_l denotes the closure) such that all the points in J' are periodic of period $p' = 2(k + 1)$

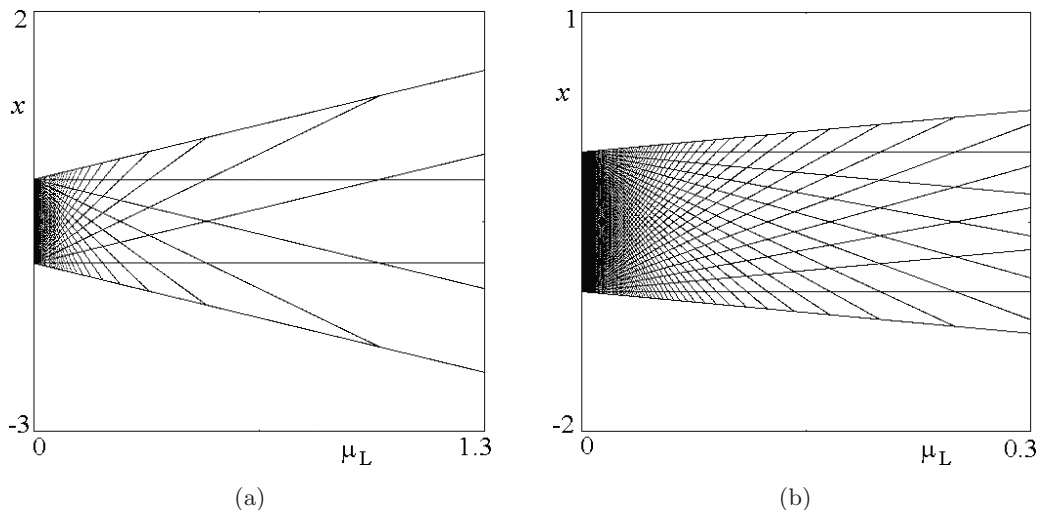


Fig. 2. (a) One-dimensional bifurcation diagram as a function of μ_L at $\mu_R = -1$. (b) An enlargement is shown.

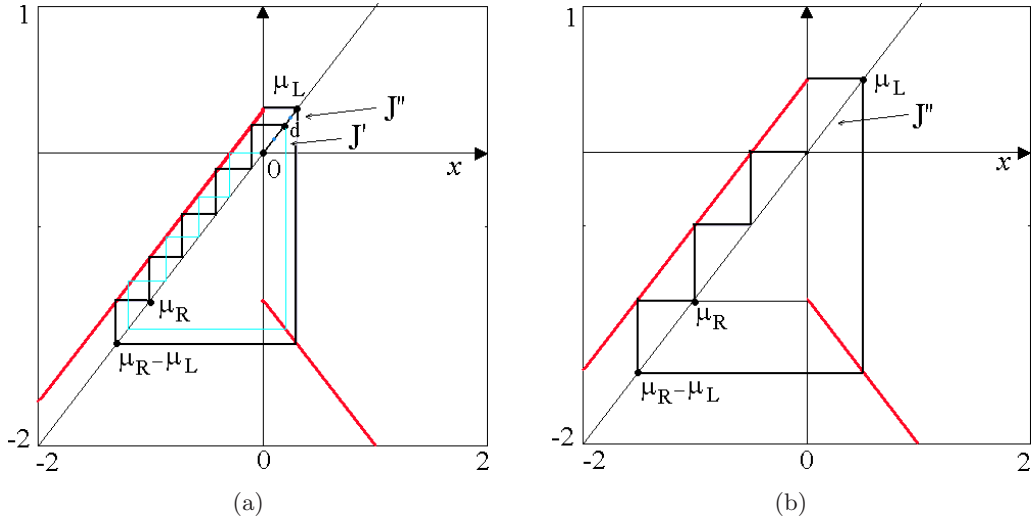


Fig. 3. Graph of the map f at $\mu_R = -1$ and (a) $\mu_L = 0.3$, (b) $\mu_L = 0.5$.

and all the points in J'' are periodic of period $p'' = 2(k + 2)$. We arrive at a BCB whenever we have an integer k such that $d = \mu_R + k\mu_L = 0$. For now, we can consider the subintervals in (16) without the critical points defining their boundaries. As we shall see below, however, we can also define them as closed intervals, specifying the behavior of the suitable choice at the discontinuity point.

We notice that the point d can also be determined as the first integer k giving a preimage (of rank $(k + 1)$) of the discontinuity point $x = 0$ in the interval J_R (i.e. the first positive preimage). That is, the first integer k such that $d = f_R^{-1} \circ f_L^{-k}(0) > 0$. In fact, given this definition, then we have $f_L^k \circ f_R(d) = 0$ which implies $-d + \mu_R + k\mu_L = 0$, from which (15) is recovered. From this, we have that each point $x < d$ takes $(k + 1)$ iterations to return to the

positive side, while a point $x > d$ takes $(k + 2)$ iterations, and, as before, $d = 0$ denotes a BCB.

In the case shown in Fig. 3(a) we have $k = 4$, thus all the points in the interval J' have prime period $p' = 10$ except for the point in the middle of the interval, which has prime period 5; while all the points in the interval J'' have prime period $p'' = 12$ except for the point in the middle of the interval, which has prime period 6. Figure 4(a) shows the related first return map. Let us prove the following:

Property 1. *Let k be the first integer such that $d = \mu_R + k\mu_L \geq 0$. When $d > 0$ then the first return map F_R is made up of two pieces with slopes -1 , defined in J' and in J'' given in (16), separated by the discontinuity point d . The intersection points with the diagonal (i.e. two fixed points of the return*

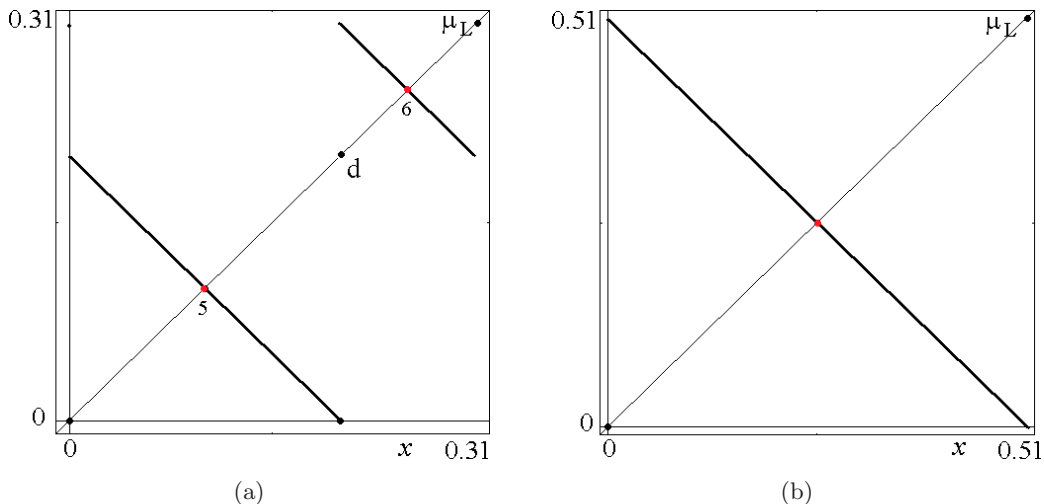


Fig. 4. Graph of the first return map F_R in the cases shown in Fig. 3, at $\mu_R = -1$ and (a) $\mu_L = 0.3$, (b) $\mu_L = 0.5$.

map F_R) are periodic points of f with prime period $(k + 1)$ in J' and $(k + 2)$ in J'' , while all the other points are periodic points of f with even periods: $2(k + 1)$ in J' and $2(k + 2)$ in J'' .

To prove this property, consider any point $x \in J'$ (and thus $d - x > 0$) then we have:

$$\begin{aligned} f_R(x) &= -x + \mu_R \in [-\mu_L + \mu_R, \mu_R] \\ f_L^k \circ f_R(x) &= -x + \mu_R + k\mu_L \\ &= -x + d > 0 \in J' \\ f_R \circ f_L^k \circ f_R(x) &= x - d + \mu_R \\ (f_L^k \circ f_R)^2(x) &= x - d + \mu_R + k\mu_L = x \end{aligned}$$

which confirms the proposition for points in J' . Similarly, let us consider any point $x \in J''$ (and thus $\mu_L - x > 0$) then we have:

$$\begin{aligned} f_R(x) &= -x + \mu_R \in [-\mu_L + \mu_R, \mu_R] \\ f_L^{k+1} \circ f_R(x) &= -x + \mu_R + (k + 1)\mu_L \\ &= -x + d + \mu_L > d \in J'' \\ f_R \circ f_L^{k+1} \circ f_R(x) &= x - d - \mu_L + \mu_R \\ (f_L^{k+1} \circ f_R)^2(x) &= x - d - \mu_L + \mu_R + (k + 1)\mu_L \\ &= x \end{aligned}$$

which confirms the proposition for points in J'' . As all the points in J' and in J'' so proved have even periods $2(k + 1)$ and $2(k + 2)$ and each periodic orbit has two points in the intervals J' and J'' , respectively, it follows that the middle points of these intervals have prime periods $(k + 1)$ and $(k + 2)$, respectively. Or also, analytically, let $x = d/2$ then

$$\begin{aligned} f_R\left(\frac{d}{2}\right) &= -\frac{d}{2} + \mu_R \\ f_L^k \circ f_R\left(\frac{d}{2}\right) &= -\frac{d}{2} + \mu_R + k\mu_L = -\frac{d}{2} + d = \frac{d}{2} \end{aligned}$$

while considering $x^* = (\mu_L + d)/2$ then we have

$$\begin{aligned} f_R(x^*) &= -x^* + \mu_R \\ f_L^{k+1} \circ f_R(x^*) &= -x^* + d + \mu_L = x^* \end{aligned}$$

which ends the proof.

Regarding the critical point d , we notice that if the point d is considered belonging to the first interval J' , defining $f(0) = f_R(0) = \mu_R$ then d is

periodic of period $2(k + 1)$, in fact:

$$\begin{aligned} f_R(d) &= -d + \mu_R \\ f_L^k \circ f_R(d) &= -d + \mu_R + k\mu_L = 0 \\ (f_L^k \circ f_R)^2(d) &= f_L^k \circ f_R(0) = f_L^k(\mu_R) \\ &= \mu_R + k\mu_L = d \end{aligned}$$

while if the point d is considered belonging to the second interval J'' , defining $f(0) = f_L(0) = \mu_L$, then d is periodic of period $2(k + 2)$, in fact:

$$\begin{aligned} f_R(d) &= -d + \mu_R \\ f_L^{k+1} \circ f_R(d) &= -d + \mu_R + (k + 1)\mu_L = \mu_L \\ (f_L^{k+1} \circ f_R)^2(d) &= f_L^{k+1} \circ f_R(\mu_L) = f_L^{k+1}(-\mu_L + \mu_R) \\ &= -\mu_L + \mu_R + (k + 1)\mu_L = d \end{aligned}$$

As stated above, a bifurcation in the periods of the first return map are associated with the trajectory of the critical point ending in the discontinuity point $x = 0$. That is, when $d = 0$ occurs. Let us prove the following:

Property 2. *Let k be the first integer such that $d = \mu_R + k\mu_L \geq 0$. When $d = 0$ then the first return map F_R is made up of one piece with slope -1 , defined in J'' . The intersection point with the diagonal (i.e. the fixed point of the return map F_R) is a periodic point of f with prime period $(k + 2)$, while all the other points are periodic points of f with even period $2(k + 2)$.*

An example is shown in Fig. 3(b), where $k = 2$, and the related first return map is shown in Fig. 4(b): All the positive points in J'' are of period $8 = 2(k + 2)$ and the point in the middle of the interval has prime period $4 = (k + 2)$. To prove Property 2 consider the point $x = \mu_L/2$, then $f_L^{k+1} \circ f_R(\mu_L/2) = \mu_L/2$, as

$$\begin{aligned} f_R\left(\frac{\mu_L}{2}\right) &= -\frac{\mu_L}{2} + \mu_R \\ f_L^{k+1} \circ f_R\left(\frac{\mu_L}{2}\right) &= -\frac{\mu_L}{2} + \mu_R + (k + 1)\mu_L \\ &= -\frac{\mu_L}{2} + \mu_L = \frac{\mu_L}{2} \end{aligned}$$

while for any other point x in $(0, \mu_L)$ we have $(f_L^{k+1} \circ f_R)^2(x) = x$, in fact,

$$\begin{aligned} f_R(x) &= -x + \mu_R \in [-\mu_L + \mu_R, \mu_R] \\ f_L^{k+1} \circ f_R(x) &= -x + \mu_R + (k + 1)\mu_L \end{aligned}$$

$$= -x + \mu_L > 0 \in J''$$

$$f_R \circ f_L^{k+1} \circ f_R(x) = x - \mu_L + \mu_R$$

$$(f_L^{k+1} \circ f_R)^2(x) = x - \mu_L + \mu_R + (k + 1)\mu_L = x$$

which ends the proof.

Regarding the critical points when we have $d = 0$, notice that defining $f(0) = f_R(0) = \mu_R$, then we have

$$f_L^k \circ f_R(0) = 0$$

and thus $d = 0$ is of period $(k + 1)$, and μ_L is preperiodic, while defining $f(0) = f_L(0) = \mu_L$, then we have

$$f_L^{k+1} \circ f_R \circ f_L(0) = 0$$

and thus in such a case we have that $d = 0$ is of period $(k + 3)$, and the trajectory includes all the critical points.

It is interesting to see that all the cycles of any period can exist, and keeping fixed μ_R the period tends to infinity as μ_L tends to 0. Moreover, as suggested by Fig. 2(a), after a specific value of μ_L the bifurcations in the periods no longer occur. In fact, we have seen that the period decreases as μ_L increases, however the value of k cannot be lower than 1, and $k = 1$ occurs whenever $\mu_L > -\mu_R$. It follows that the last BCB takes place when $\mu_L = -\mu_R$ giving $d = 0$ for $k = 1$ [see an example in Fig. 5(a)]. Then for any higher value of μ_L , we always have that the image of $\mu_R, f_L(\mu_R)$, enters J_R in one iteration, and thus $k = 1$. This means that

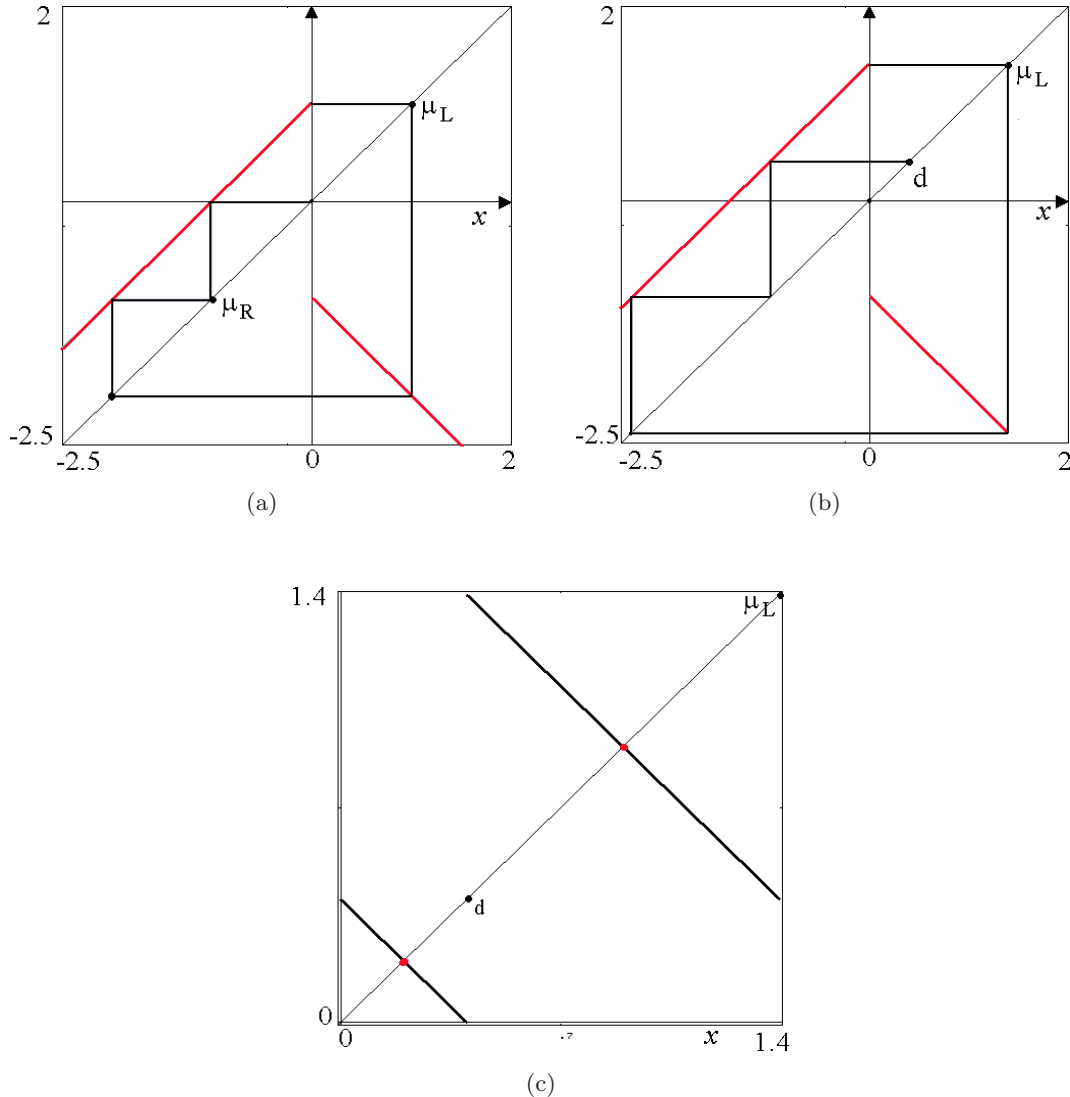


Fig. 5. (a) Graph of the map f at $\mu_L = -\mu_R$, and $\mu_R = -1$. (b) Graph of the map f at $\mu_R = -1$ and $\mu_L = 1.4$ for which $k = 1$. (c) The related first return map is shown.

the simplest situation consists of points belonging to 4-cycles in J' (a 2-cycle in the middle point), and points of 6-cycles in J'' (a 3-cycle in the middle point). A qualitative picture of this simplest case is shown in Fig. 5(b) and the related first return map in J_R is shown in Fig. 5(c).

As well, we note that all the preperiodic points of the cycles can be easily obtained by taking the preimages f of the intervals J' and J'' .

Summarizing, we have so proved the following theorem.

Theorem 1. *Let $a_R = -1$, $a_L = 1$, $\mu_R < 0$ and $\mu_L > 0$, $I = [-\mu_L + \mu_R, \mu_L]$, $K = -(\mu_R/\mu_L)$. If K is not an integer, let $k = \lfloor K \rfloor + 1$, then $d = \mu_R + k\mu_L > 0$, $J' \cup J'' =]0, d[\cup]d, \mu_L[$, and Property 1 holds (all the points in J' are $2(k + 1)$ -cycles and the middle point $d/2$ is a $(k + 1)$ -cycle, while all the points in J'' are $2(k + 2)$ -cycles and the middle point $x^* = (\mu_L + d)/2$ is a $(k + 2)$ -cycle). When $k = K$ is an integer then $d = \mu_R + k\mu_L = 0$, a BCB occurs and Property 2 holds (all the points in J'' are $2(k + 2)$ -cycles and the middle point $x^* = (\mu_L + d)/2$ is a $(k + 2)$ -cycle). The critical points and the periodic points cover the whole interval I . On the real line, the preperiodic points of the cycles in I are obtained by the preimages of the points in I .*

4. Particular Case $a_R a_L = 0$

Here, we consider the particular case in which one of the functions defining the map is constant. Let us assume $a_R = 0$, as the other case comes from

the property in (3). In this section, we consider the map

$$x' = f(x) = \begin{cases} f_L(x) = a_L x + \mu_L, & \text{if } x < 0 \\ f_R(x) = \mu_R, & \text{if } x > 0 \end{cases} \quad (17)$$

where $\mu_R < 0$ and $\mu_L > 0$. As any point on the right-hand side is mapped into a unique point ($\mu_R < 0$), it follows that we only have to consider the trajectory of this point. Obviously, when not divergent, i.e. when (5) holds, $\mu_L/(1 - a_L) < \mu_R$, this trajectory is periodic and the only question is of which period. This information is given immediately by the first return map, which completely explains this case, and the related BCB curves, which can be seen in Fig. 6.

In Fig. 6 the region with negative values of a_L is not represented because, as we shall see in the next section, that region only includes a stable 2-cycle or divergence. The integer that gives the period of the trajectories is obtained by the trajectory of the critical point μ_R : since $f_L(x) = \mu_R$ for any $x > 0$, we apply the map f_L to the point μ_R as long as we have a positive point again (no matter which one it is), thus from

$$\begin{aligned} f_L^k \circ f_R(0) &= f_L^k(\mu_R) \\ &= a_L^k \mu_R + \mu_L \frac{1 - a_L^k}{1 - a_L} & \text{if } a_L \neq 1 \\ f_L^k \circ f_R(0) &= f_L^k(\mu_R) \\ &= \mu_R + k\mu_L & \text{if } a_L = 1 \end{aligned} \quad (18)$$

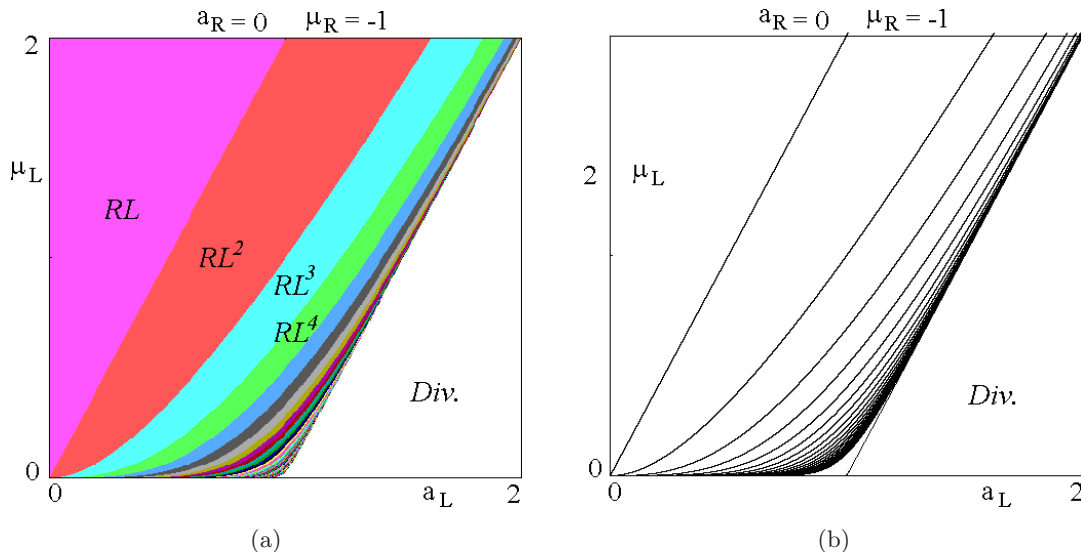


Fig. 6. (a) Two-dimensional bifurcation diagram at $a_R = 0$ and $\mu_R = -1$. (b) The analytical BCB curves that bound the stability regions of the cycles with symbol sequence RL^k , for $k = 1, \dots, 20$.

let $k \geq 1$ be the first integer such that $f_L^k(\mu_R) > 0$, then we have a $(k + 1)$ -cycle. The curve of equation $f_L^k(\mu_R) = 0$, that is:

$$a_L^k \mu_R + \mu_L \frac{1 - a_L^k}{1 - a_L} = 0, \quad \text{if } a_L \neq 1 \tag{19}$$

$$\mu_R + k \mu_L = 0, \quad \text{if } a_L = 1$$

denotes a BCB from the region of a $(k + 1)$ -cycle to that of a $(k + 2)$ -cycle. In the region in which $f_L^k(\mu_R) > 0$ the dynamics of the map f converge to a $(k + 1)$ -cycle. In Fig. 6(b) we show a few BCB curves (for $k = 1, \dots, 20$). The limit set of these BCB curves, as $k \rightarrow \infty$, is the equation

$$\mu_L = \mu_R(1 - a_L) \tag{20}$$

which corresponds to the contact bifurcation given in (9) after which (for $\mu_L < \mu_R(1 - a_L)$) we have a region associated with divergent dynamics for f .

5. Generic Case

In this section, we consider the generic case which is the main object of this work. In order to describe the BCB curves, let us first show a figure that summarizes the properties of our map. In Fig. 7, we show the regions associated with attracting periodic orbits in the parameter plane (a_R, a_L) . As the figure refers to the case where $\mu_R = -1$ and $\mu_L = 1$ are the bifurcation curves and the colored regions (denoting attracting cycles of different periods) are completely symmetric with respect to the main diagonal. When

an asymmetry appears it refers to the coexistence of stable cycles, i.e. overlapping of periodicity regions (as the initial condition is kept as the same point $x_0 = -0.001$). The similar figures at different values of μ_R and μ_L clearly do not have this symmetric shape, and the regions are slightly deformed, keeping in any case the same main qualitative properties, in particular, those of the points denoted by P_n , although the overlapping regions may change their shape. In each portion of the parameter plane of Fig. 7(a) we simply illustrate the qualitative shape of the map in the related quadrant.

5.1. Positive quadrant

We recall that in the positive quadrant as long as $0 < a_R < 1$ and $0 < a_L < 1$, we have stable cycles of any period, associated with the well-known *period adding* rule (examples of some particular maps can be found in [Avrutin & Schanz, 2006, 2008]), and the related BCB curves, characterizing the appearance/disappearance of cycles, are given in analytic form for several levels of complexity in [Gardini *et al.*, 2010; Avrutin *et al.*, 2010b], and the formulas there given can also be applied for higher complexity levels, which explains the BCB curves in that portion of phase plane. For each fixed constellation of the parameters only one stable cycle can exist, or none (when quasiperiodic trajectories occur). As long as the parameters satisfy the condition $\mu_L(1 - a_R) - \mu_R(1 - a_L) > 0$, none of the periodicity regions ever overlap. In Fig. 7, this inequality

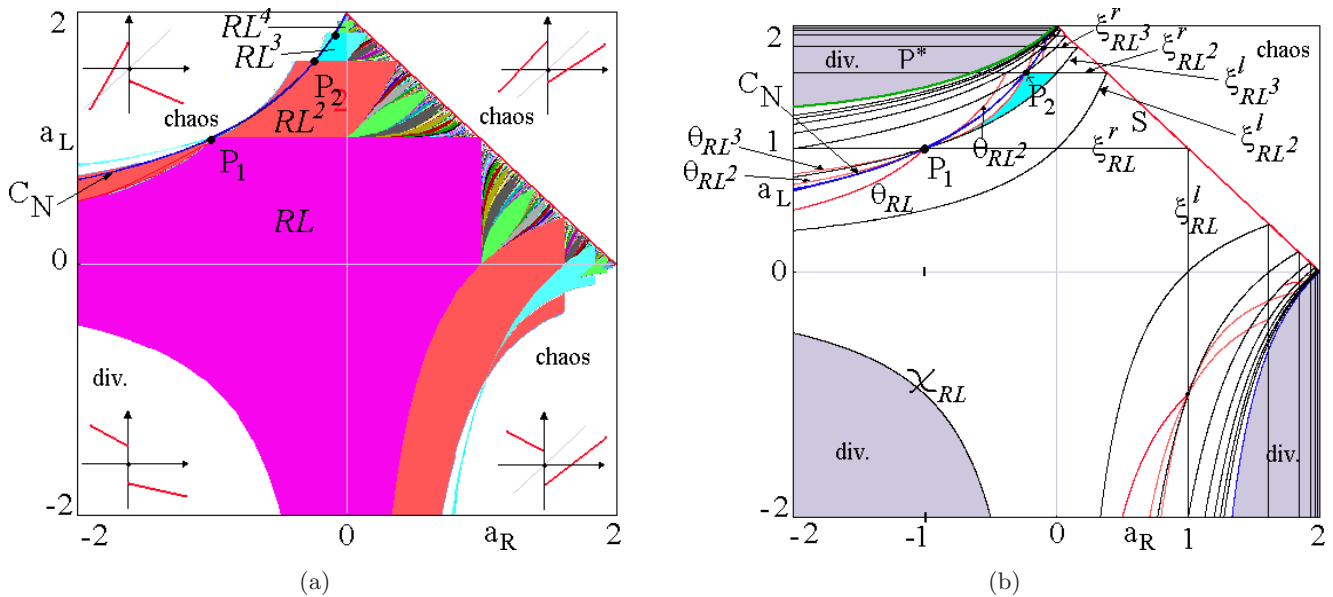


Fig. 7. (a) Two-dimensional bifurcation diagram numerically obtained, with stable periodicity regions in different colors. (b) A few BCB curves are drawn, the equations for which are given in the text.

corresponds to the region of the positive quadrant below the set (S) of equation

$$(S): \mu_L(1 - a_R) - \mu_R(1 - a_L) = 0 \quad (21)$$

Crossing this set, the map turns from invertible in the invariant absorbing interval $[\mu_R, \mu_L]$ into nonuniquely invertible. The region below the set (S) is called the stability region in [Gardini *et al.*, 2010], where it is also proved that each pair of the infinitely many BCB curves associated with each periodicity region intersect in points of the set (S) where a stability change occurs. For parameters above (S) , infinitely many unstable cycles exist, and the dynamics are chaotic, with robust chaos in cyclical intervals. In that region the BCB are responsible for the changes in the cyclical chaotic intervals, also called chaotic band and band merging bifurcations, as described in [Avrutin *et al.*, 2007, 2008a, 2008b, 2009; Avrutin *et al.*, 2010c].

A bounded chaotic attractor exists up to the final bifurcation leading to divergence of the generic trajectory. This occurs when the parameters cross the bifurcation curves associated with the contact of the invariant interval with an unstable fixed point of f .

The boundaries of the BCB curves of the periodicity regions of first level of complexity associated with the so-called *maximal cycles*, or *principal cycles*, will be recalled below, as they also intersect the region of interest here, the one with $a_R < 0$.

As we can see from Fig. 7, on the sets $a_R = 0$ and $a_L = 0$ of the parameter space we have only contiguous regions of stable cycles of increasing period, one after the other. This reflects the property proved in the previous section.

5.2. Stability region of the 2-cycle

We describe here, the wide periodicity region associated with the 2-cycle, whose periodic points $x_0^* > 0$ and $x_1^* < 0$ are given by

$$x_0^* = \frac{a_L \mu_R + \mu_L}{1 - a_R a_L} > 0, \quad x_1^* = \frac{a_R \mu_L + \mu_R}{1 - a_R a_L} < 0 \quad (22)$$

The two BCB curves, due to the merging of the periodic points with the discontinuity point in $x = 0$, are given by:

$$\xi_{RL}^r: a_L \mu_R + \mu_L = 0, \quad \xi_{RL}^l: a_R \mu_L + \mu_R = 0 \quad (23)$$

(the straight lines of equation $a_L = -(\mu_L/\mu_R)$ and $a_R = -(\mu_R/\mu_L)$ in Fig. 7). The 2-cycle is stable

as long as $|a_R a_L| < 1$ and becomes unstable via a degenerate flip-bifurcation when the parameters satisfy the equation

$$\theta_{RL}: a_R a_L = -1 \quad (24)$$

which gives the two portions of hyperbola in red in Fig. 7, and a portion of the existence region is associated with an unstable 2-cycle. Moreover, the boundary of the stability region of the 2-cycle in the lower left portion of the parameter plane ($a_R < 0$ and $a_L < 0$) is the curve of equation

$$\chi_{RL}: a_R a_L = 1 \quad (25)$$

which corresponds to the merging of the 2-cycle with a point on the Poincaré Equator, at infinity. In fact, as we can see from (22), the coordinates of the periodic points of the 2-cycle tend to infinity as $a_R a_L$ tends to 1, after which (for $a_R a_L > 1$) no cycle exists in the real line, and the dynamics are all divergent (similar bifurcations are described in [Avrutin *et al.*, 2010a]).

We recall that all the flip bifurcations occurring in piecewise linear maps to a k -cycle are *degenerate* (see also [Sushko & Gardini, 2010]) which means that at the bifurcation value a segment of the real line exists in which all the points are $2k$ -cycles, with the bifurcating k -cycle inside. After the flip bifurcation, all such $2k$ -cycles disappear, leaving only one unstable k -cycle. The cycle which bounds the interval at the bifurcation value also undergoes a *border collision*. The dynamics occurring after the degenerate flip bifurcation depend on the shape of the map in the other part of the segment of cycles.

5.3. Region with $a_L a_R < 0$

In Sec. 2 we have already remarked that contact bifurcations leading to almost all divergent trajectories occur when the invariant interval $I = [a_R \mu_L + \mu_R, \mu_L]$ has a contact with the unstable fixed point P^* . The curve given in (9) associated with the “*final bifurcation*” is also drawn in Fig. 7(b) (green arc of curve), bounding the regions of mainly divergent dynamics in the upper left portion of the phase plane. This bifurcation is the border collision bifurcation of the critical point (lower boundary of I) with the unstable fixed point P^* (also homoclinic bifurcation of P^*).

From the same picture it is clear that the infinitely many periodicity regions existing for $0 < a_R < 2$ and $0 < a_L < 2$ issue from particular points on the axes $a_R = 0$ and $a_L = 0$, which are

also points of intersection of two periodicity regions of maximal cycles. Crossing such axes and entering the region $a_L a_R < 0$, the periodicity regions of the maximal cycles intersect in pair, that is, for any $k \geq 2$ the periodicity region of the k -cycle intersects the region of the $(k + 1)$ -cycle, and for each cycle there exists a region in which it is the only stable one, without overlapping other stable periodicity regions. This was already determined for particular families of maps in [Avrutin *et al.*, 2006]. Here, we consider the generic map in standard form, in order to give an analytical proof of this and other properties by using the first return map F_R , which will be considered in the following subsections.

5.3.1. BCB curves

The reason why we limit our interest here only to the regions of cycles of first complexity level is that they are the only cycles which may be stable when $a_R a_L < 0$. Let us recall that in the particular cases $a_R a_L = 0$, as we have seen in Sec. 4, only these cycles exist, and their boundaries represent intersection points of two different BCB curves, denoting the intersection of periodicity regions crossing from $a_R a_L > 0$ to $a_R a_L < 0$. The periodicity regions associated with these stable periodic orbits of increasing periods are bounded by BCB curves whose analytic expression is easy to obtain. Such cycles have the simplest structure, obtained when we apply in order the maps with symbol $RL \cdots L$. This is a *simple* case because in this way we can simply order the periodic points, and easily perform the related computations. For a cycle of period $(n + 1)$ let us call the related periodic points as $0 < x_0^* < \mu_L$ and $x_1^* < \cdots < x_n^* < 0$. Then the periodic points of the cycle are fixed points of the iterated map $f^{n+1}(x)$ and x_0^* is the fixed point of the linear function $f_L^n \circ f_R(x)$, which is a periodic point for $f(x)$ as long as

$$0 \leq x_0^* \leq \mu_L$$

and the conditions $x_0^* = 0$ and $x_0^* = \mu_L$ (this one corresponds to $x_n^* = 0$) determine the BCB curves. Then from:

$$\begin{aligned}
 f_L^n \circ f_R(x) &= (a_L^n a_R)x \\
 &+ \left(\mu_R a_L^n + \mu_L \frac{1 - a_L^n}{1 - a_L} \right) \quad \text{if } a_L \neq 1 \\
 f_L^n \circ f_R(x) &= a_R x + \mu_R + n \mu_L \quad \text{if } a_L = 1
 \end{aligned}$$

by using the equality $x_0^* = f_L^n \circ f_R(x_0^*)$ we obtain the periodic point:

$$0 \leq x_0^* = \frac{a_L^n (\mu_R + \mu_L \phi_n^L)}{1 - a_L^n a_R} \leq \mu_L \tag{26}$$

where

$$\begin{aligned}
 \phi_n^L &= \frac{1 - a_L^n}{(1 - a_L) a_L^n} \quad \text{if } a_L \neq 1, \\
 \phi_n^L &= n \quad \text{if } a_L = 1.
 \end{aligned} \tag{27}$$

Notice that in the region we are interested in ($a_R < 0$ and $a_L > 0$), the denominator in (26) is always positive. We denote by $\xi_{RL^n}^r$ (resp. $\xi_{RL^n}^l$) the BCB curve obtained due to the merging of a periodic point of the orbit with the discontinuity point $x = 0$ from the right (resp. left) side. That is, the BCB curve $\xi_{RL^n}^r$ is the BCB curve obtained due to the merging $x_0^* = 0$, while $\xi_{RL^n}^l$ is the BCB curve obtained due to the merging $x_n^* = 0$ which also corresponds with $x_0^* = \mu_L$. Thus the two BCB curves are obtained due to the merging of the periodic point x_0^* with the boundaries of its existence interval. From $0 \leq x_0^* \leq \mu_L$ we get:

$$\begin{aligned}
 a_L^n (\mu_R + \mu_L \phi_n^L) - \mu_L (1 - a_L^n a_R) &\leq 0 \\
 a_L^n (\mu_R + \mu_L \phi_n^L) &\geq 0
 \end{aligned}$$

so that the BCB curves are:

$$\xi_{RL^n}^l: a_L^n (\mu_R + \mu_L \phi_n^L) - \mu_L (1 - a_L^n a_R) = 0 \tag{28}$$

$$\xi_{RL^n}^r: \mu_R + \mu_L \phi_n^L = 0 \tag{29}$$

It is plain that the eigenvalue of a cycle is given by the product of the slopes of the linear maps which are applied in the cycle. So this $(n + 1)$ -cycle becomes unstable via degenerate flip when

$$\theta_{RL^n}: a_L^n a_R = -1 \tag{30}$$

denoting the flip-bifurcation curves.

In Fig. 7(b) we have drawn a few BCB curves $\xi_{RL^n}^r$ (horizontal lines in that projection) and $\xi_{RL^n}^l$ in black, together with a few flip-curves θ_{RL^n} in red. In the upper left part, it can be seen that all three involve (intersect), a particular blue curve there reported, and also shown in Fig. 7(a). This curve represents the transition of the map f from invertible in the absorbing interval $I = [a_R \mu_L + \mu_R, \mu_L]$ to noninvertible in that interval. The map $f(x)$ is invertible as long as $f_L(a_R \mu_L + \mu_R) > \mu_R$ so that the set (C_N) — crossing which the map becomes non-uniquely invertible — is given by $f_L(a_R \mu_L + \mu_R) = \mu_R$ that is:

$$C_N: \mu_L (1 + a_L a_R) + \mu_R (a_L - 1) = 0. \tag{31}$$

The similar transition when the slopes are positive is given by the set (S) defined in (21). As already remarked, in that region the crossing of the set (S) represents a drastic transition from only stability to only robust chaos. This is not the case when the slopes satisfy $a_R a_L < 0$. In fact, it is easy to see that in Fig. 7(a) above the set C_N there is a white region (associated with chaotic dynamics) followed by a small portion of stability of the 4-cycle.

It is worth noticing also that the set C_N intersects all the BCB curves $\xi_{RL^n}^r$ exactly at the points belonging to the flip bifurcation curves of cycles with the symbolic sequence RL^{n+1} existing above that curve. The BCB curve $\xi_{RL^{n+2}}^l$ also crosses at this point. This is not numerical evidence, and the following Property will be used later:

Property 3. *Let $P_n \in \xi_{RL^n}^r \cap \theta_{RL^{n+1}}$ for $n \geq 1$, then $P_n \in C_N$ and $P_n \in \xi_{RL^{n+2}}^l$.*

In fact, from (30) we have $a_L^n = -1/(a_L a_R)$, and from (29) and (27), substituting:

$$\mu_R + \mu_L \frac{a_L a_R + 1}{a_L - 1} = 0$$

from which the expression in (31) is recovered. After some algebra it can be seen that also the equation of $\xi_{RL^{n+2}}^l$ is satisfied. The computations with the formulas given in (28) are not easy, but in the next subsection we shall give a different expression of the same bifurcation curve, with which the proofs follow soon.

Another peculiarity of the flip-bifurcation curves is that those associated with the cycles of period 3 and 4 intersect each other and exchange at a very particular point, when $a_L = 1$ and $a_R = -1$. This is immediate from their equations in (30). Indeed the same property holds for any flip-curve, but for the other cycles it is not dynamically relevant because the flip-curves cannot exit from the existence region, and the parameter point $(a_R, a_L) = (-1, 1)$ belongs to the existence regions of the cycles of periods 2, 3, 4 only. *The property which holds iteratively for all the cycles existing for $a_L > 1$ is the one noted in Property 3, that is, a flip bifurcation curve $\theta_{RL^{n+1}}$ that starts from the BCB curve $\xi_{RL^{n+1}}^r$ crosses through $\xi_{RL^n}^r$ at the point P_n and ends in the BCB curve $\xi_{RL^{n+1}}^l$.*

5.3.2. Use of the first return map

We describe here a different (and useful) approach to study the bifurcations in the case of slopes with

opposite sign, for which a first return map F_R is well defined. As we have seen, when an invariant absorbing interval $I = [a_R \mu_L + \mu_R, \mu_L]$ exists, it is not possible to apply the function on the right side for two consecutive iterations. In fact, whenever we consider a positive point $x > 0$, then we have $f_R(x) < 0$. This allows us to a correct definition of the first return map. Let $J_R = [0, \mu_L] = I \cap \{x \geq 0\}$ then we can simply construct the *first return map* in J_R , as

$$F_R: x \in J_R \rightarrow f^m(x) \in J_R$$

where m is the first integer for which $f^m(x) \in J_R$, and this map describes all the bifurcations (including the BCB) of the map f in I . As f is discontinuous with a discontinuity point in $x = 0$, which means that points in a neighborhood of $x = 0$ are subject to different functions, a similar fate will occur also to points on opposite sides of the preimages of the discontinuity point $x = 0$, depending on the side to which they belong. The preimages of the discontinuity point $x = 0$ must necessarily be taken first with the left side, i.e. with f_L^{-1} as long as we obtain a point in the range of f_R to which we can apply f_R^{-1} reaching the side $x > 0$. Thus, as seen in Sec. 3, an important integer is the first k , necessarily $k \geq 1$, such that

$$d_k = f_R^{-1} \circ f_L^{-k}(0) > 0 \tag{32}$$

and clearly, once a first preimage d_k exists, then also

$$d_{k+j} = f_R^{-1} \circ f_L^{-(k+j)}(0) > 0, \quad \forall j \geq 1 \tag{33}$$

exist as preimages of the origin on the R side, as the preimages $f_L^{-(k+j)}(0)$ tend to the unstable fixed point P^* as j tends to ∞ , when P^* exists (i.e. for $a_L > 1$), otherwise, the preimages tend to $-\infty$. To understand the dynamics of $f(x)$, however, we are only interested in the points d_{k+j} belonging to (or entering inside) the interval domain of $F_R: J_R = [0, \mu_L]$.

It is plain that for the first return map F_R , d_k must be a discontinuity point, and points in $0 < x < d_k$ will take $(k + 1)$ iterations in order to be positive again, while points in a right neighborhood of d_k , between d_k and d_{k+1} , will take $(k + 2)$ iterations.

Thus it is easy to see that an important bifurcation occurs whenever we have $d_k = \mu_L$ as this denotes that the discontinuity point of the first return map F_R is entering the interval J_R [see Figs. 8(a) and 8(b)], and a bifurcation also occurs whenever we have $d_k = 0$, as this denotes that the

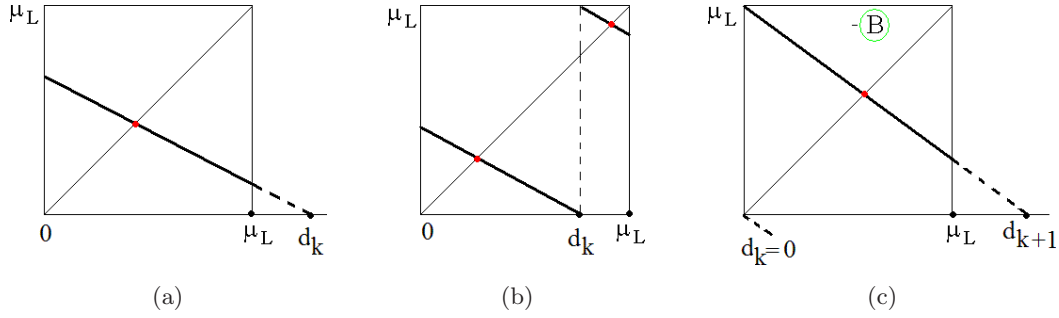


Fig. 8. Qualitative shapes of the first return map F_R . The case shown in (c) corresponds to point (B) in Fig. 10.

discontinuity point of the first return map F_R is exiting from the interval J_R [see Fig. 8(c)]. Clearly both these bifurcations cause a change in the definition of the first return map, as the number of iterations to be applied to f_L^{-1} in order to get the first preimage of the origin on the positive side is changed.

From the definition of d_k in (32) we also have $f_L^k \circ f_R(d_k) = 0$, thus considering the function $f_L^k \circ f_R(x) = (a_L^k a_R)x + a_L^k(\mu_R + \mu_L \phi_k^L)$, from $f_L^k \circ f_R(d_k) = 0$ we obtain:

$$d_k = \frac{\mu_R + \mu_L \phi_k^L}{-a_R} \tag{34}$$

So that defining $T_0(x) = f_L^k \circ f_R(x)$ then $T_0(x)$ represents the first return map for $0 < x < d_k$, and we have to consider $T_1(x) = f_L^{k+1} \circ f_R(x)$ as the first return function for $d_k < x < d_{k+1}$. Thus, when $0 < d_k < \mu_L < d_{k+1}$ we have a well defined map [see Fig. 8(b)]:

$$F_R(x) = \begin{cases} T_0(x) = f_L^k \circ f_R(x) \\ \quad = a_L^k(a_R x + \mu_R + \mu_L \phi_k^L), \\ \quad \quad \quad \text{if } 0 \leq x < d_k \\ T_1(x) = f_L^{k+1} \circ f_R(x) \\ \quad = a_L^{k+1}(a_R x + \mu_R + \mu_L \phi_{k+1}^L), \\ \quad \quad \quad \text{if } d_k < x \leq \mu_L \end{cases} \tag{35}$$

The components are both decreasing functions, as the slopes of T_0 and T_1 are negative, and the fixed points of F_R are periodic points of $f(x)$. Say

$$\begin{aligned} x_0^* &= \frac{a_L^k(\mu_R + \mu_L \phi_k^L)}{1 - a_L^k a_R}, \\ x_1^* &= \frac{a_L^{k+1}(\mu_R + \mu_L \phi_{k+1}^L)}{1 - a_L^{k+1} a_R} \end{aligned} \tag{36}$$

the fixed points of $T_0(x)$ and $T_1(x)$, respectively. Then x_0^* is a periodic point belonging to the cycle of period $(k + 1)$ of $f(x)$. The first and unique point on the R side of the cycle with symbolic sequence RL^k , and eigenvalue $\lambda_{k+1} = a_L^k a_R < 0$. The fixed point x_1^* is a periodic point of $f(x)$ belonging to the cycle of period $(k + 2)$, while the first and unique point on the R side of the cycle with symbolic sequence RL^{k+1} having eigenvalue $\lambda_{k+2} = a_L^{k+1} a_R = a_L \lambda_{k+1} < 0$. The following iterative properties derive immediately from the definitions:

Property 4

$$\phi_{k+1}^L = \phi_k^L + \frac{1}{a_L^{k+1}} \tag{37}$$

$$d_{k+1} = d_k + \frac{\mu_L}{-a_R a_L^{k+1}} = d_k + \frac{\mu_L}{|\lambda_{k+2}|} \tag{38}$$

Notice that the ranges of the two functions defined in (35) are given by:

$$T_0([0, d_k]) = [a_L^k(\mu_R + \mu_L \phi_k^L), 0] = [-a_L^k a_R d_k, 0] \tag{39}$$

(as $T_0(0) = a_L^k(\mu_R + \mu_L \phi_k^L)$ and $T_0(d_k) = 0$) and from $T_1(d_k) = a_L^{k+1}(a_R d_k + \mu_R + \mu_L \phi_{k+1}^L) = a_L^{k+1}(-\mu_R - \mu_L \phi_k^L + \mu_R + \mu_L \phi_{k+1}^L) = a_L^{k+1} \mu_L (\phi_{k+1}^L - \phi_k^L) = \mu_L$, we have:

$$\begin{aligned} T_1([d_k, \mu_L]) &= [\mu_L, T_1(\mu_L)] \\ &= [\mu_L, a_L^{k+1}(a_R \mu_L + \mu_R + \mu_L \phi_{k+1}^L)] \end{aligned} \tag{40}$$

As already noted, the two functions T_0 and T_1 given above *in general* define a first return map, i.e. when $0 < d_k < \mu_L < d_{k+1}$, but bifurcations occur whenever the intervals defined in (39) and (40) reduce to a point, that is:

- (i) when $d_k = 0$, as the cycle of period $(k + 1)$ with symbol sequence RL^k disappears/appears

from J_R , which gives the BCB curves $\xi_{RL^k}^r$ of equation $\mu_R + \mu_L \phi_k^L = 0$ given in (29), and (ii) when $f_L^{k+1} \circ f_R(\mu_L) = \mu_L$, as the cycle of period $(k + 2)$ with symbol sequence RL^{k+1} appears/disappears from J_R , which gives

$$\xi_{RL^{k+1}}^r: a_L^{k+1}(a_R \mu_L + \mu_R + \mu_L \phi_{k+1}^L) - \mu_L = 0$$

corresponding to the BCB curves $\xi_{RL^{k+1}}^l$ given in (28). But note that $f_L^{k+1} \circ f_R(\mu_L) = \mu_L$ means $f_L(f_L^k \circ f_R(\mu_L)) = \mu_L$ and this occurs iff $f_L^k \circ f_R(\mu_L) = 0$ (that is iff $d_k = \mu_L$). Thus the BCB curves $\xi_{RL^{k+1}}^l$ also have a simpler equation (considering $f_L^k \circ f_R(\mu_L)$ from (35)), given by:

$$\xi_{RL^{k+1}}^l: a_R \mu_L + \mu_R + \mu_L \phi_k^L = 0 \quad (41)$$

To be also more explicit the proof is as follows:

$$a_L^{k+1}(a_R \mu_L + \mu_R + \mu_L \phi_{k+1}^L) - \mu_L = 0$$

$$a_R = \frac{\mu_L - a_L^{k+1}(\mu_R + \mu_L \phi_{k+1}^L)}{a_L^{k+1} \mu_L}$$

$$a_R = \frac{1}{a_L^{k+1}} - \frac{\mu_R}{\mu_L} - \phi_{k+1}^L$$

$$a_R = -\frac{\mu_R}{\mu_L} - \phi_k^L$$

$$\mu_R + \mu_L \phi_k^L + a_R \mu_L = 0$$

We have so proved the following.

Theorem 2. Let $a_R < 0, a_L > 0, \mu_R < 0$ and $\mu_L > 0$. Let $d_k = f_R^{-1} \circ f_L^{-k}(0) = (\mu_R + \mu_L \phi_k^L) / -a_R$ be the first preimage of the discontinuity point $x = 0$ on the positive side R . Then the BCB curves of the cycles of first complexity level are given by

$$\begin{aligned} \xi_{RL^{k+1}}^l: d_k &= \mu_L \quad (\text{i.e. } \mu_R + \mu_L \phi_k^L + a_R \mu_L = 0) \\ \xi_{RL^k}^r: d_k &= 0 \quad (\text{i.e. } \mu_R + \mu_L \phi_k^L = 0) \end{aligned} \quad (42)$$

where ϕ_k^L is defined in (27):

$$\phi_k^L = \frac{1 - a_L^k}{(1 - a_L)a_L^k} \quad \text{if } a_L \neq 1,$$

$$\phi_k^L = k \quad \text{if } a_L = 1$$

We recall that by using the equations given in (42) the algebraic steps to prove Property 3 are quickly derived.

Let us also notice that the two different dynamic behaviors observed in Fig. 7 crossing the point $(a_R, a_L) = (-1, 1)$ have a clear interpretation in the first return map F_R . In fact, from $\lambda_{k+2} = a_L^{k+1} a_R = a_L \lambda_{k+1}$ we immediately have the following property characterizing the flip bifurcations:

Property 5

- (j) If $a_L < 1$ then $\lambda_{k+1} < \lambda_{k+2} = a_L \lambda_{k+1}$ and thus for a transition in which a_R is decreasing, the degenerate flip bifurcation of the cycle RL^k of lower period occurs first (i.e. before that of cycle RL^{k+1}) [Fig. 9(a)];
- (jj) if $a_L > 1$ and $-1 < a_R < 0$ then $\lambda_{k+2} = a_L \lambda_{k+1} < \lambda_{k+1}$ and thus for decreasing a_R the degenerate flip bifurcation of the cycle RL^{k+1} of higher period occurs before that of the cycle RL^k . (Fig. 9(b), corresponding to point A in Fig. 10);
- (jjj) the degenerate flip bifurcations of two coexisting cycles occur simultaneously iff $a_L = 1$ and $a_R = -1$.

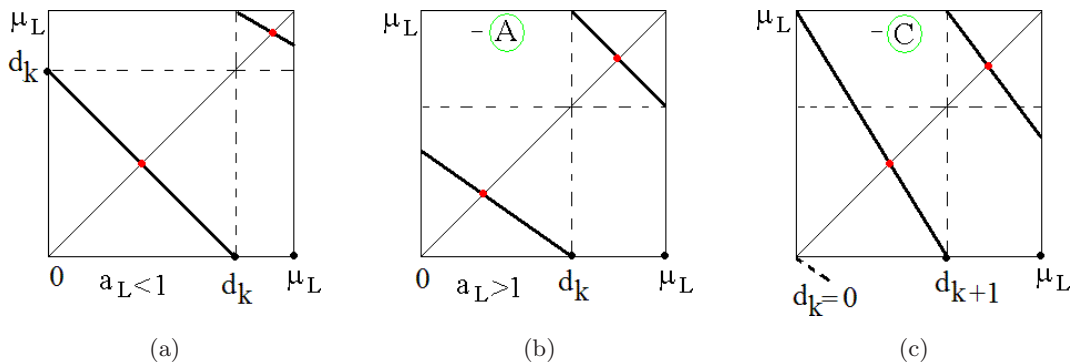


Fig. 9. Qualitative shapes of the first return map F_R . The case shown in (b) corresponds to point (A) in Fig. 10, while the one in (c) corresponds to point (C) in Fig. 10.

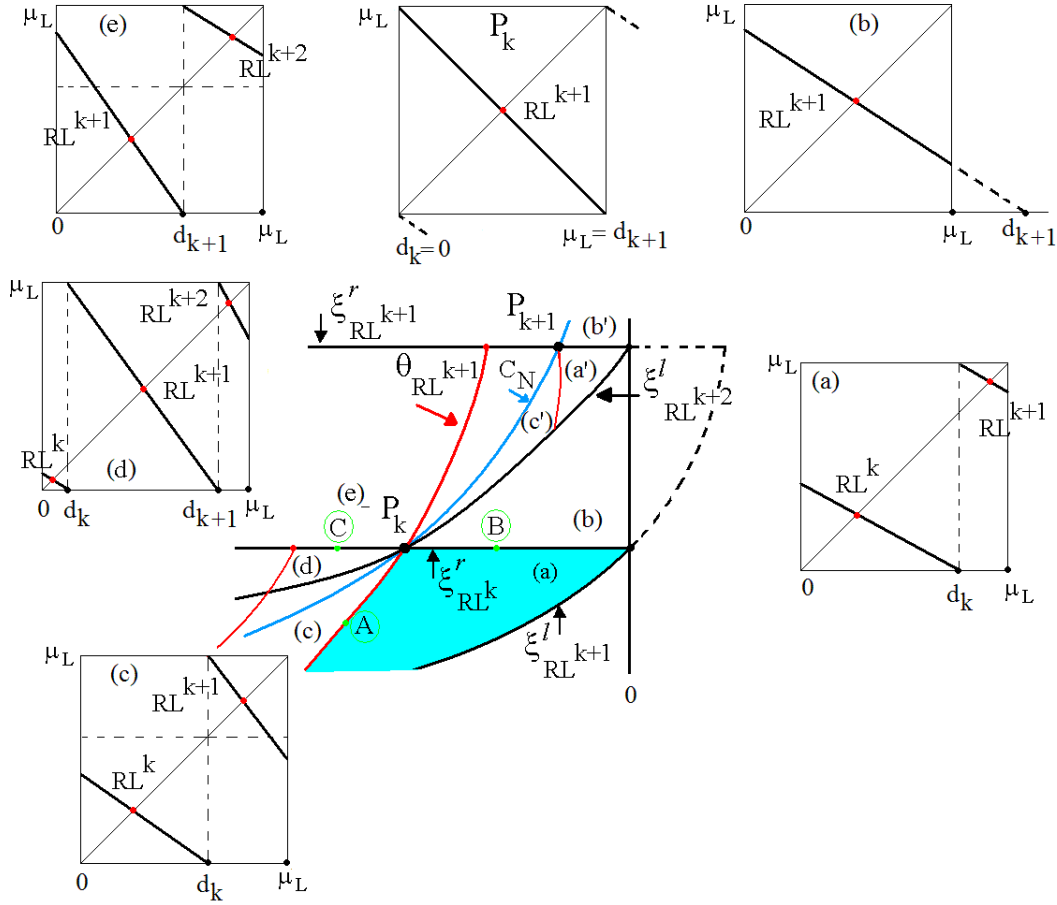


Fig. 10. Qualitative behavior of the first return map in the different regions bounded by the bifurcations curves. The light blue region qualitatively represents the corresponding light blue region for $k = 2$ in the parameter plane in Fig. 7(b).

The case in (jjj), due to $\lambda_{k+2} = \lambda_{k+1} = -1$, corresponds to the particular case fully considered in Sec. 3.

The following properties characterize the crossing of a parameter point through a BCB curve $\xi_{RL^k}^r$.

Property 6. Let the parameters (a_R, a_L, μ_R, μ_L) satisfy $d_k = 0$ then

$$d_{k+1} = \frac{\mu_L}{-a_L^{k+1} a_R} = \frac{\mu_L}{|\lambda_{k+2}|} \quad (43)$$

$$T_1(\mu_L) = \mu_L(1 - |\lambda_{k+2}|) \quad (44)$$

In fact, at a bifurcation value due to $d_k = 0$ from (38) we have immediately the expression of d_{k+1} , which proves (43). While from (35) by using (37) we have:

$$\begin{aligned} T_1(\mu_L) &= a_L^{k+1}(a_R \mu_L + \mu_R + \mu_L \phi_{k+1}^L) \\ &= a_L^{k+1} a_R \mu_L + a_L^{k+1}(\mu_R + \mu_L \phi_k^L) + \mu_L \end{aligned}$$

$$\begin{aligned} &= a_L^{k+1} a_R \mu_L - a_L^{k+1} a_R d_k + \mu_L \\ &= \mu_L(1 - |\lambda_{k+2}|) \end{aligned} \quad (45)$$

which proves (44).

The particular expressions so determined are used to prove the following.

Property 7. Let the parameters (a_R, a_L, μ_R, μ_L) satisfy $d_k = 0$ (and thus belonging to the BCB curve $\xi_{RL^k}^r$ associated with the cycle RL^k) then:

- (1) If the cycle RL^{k+1} is stable then we have $T_1(\mu_L) > 0$ and $d_{k+1} = \mu_L/(|\lambda_{k+2}|) > \mu_L$, which means that there are no discontinuity points inside the interval J_R , thus the map F_R (and f) is invertible: the existing cycle RL^{k+1} is globally attracting, and the return map F_R is continuous (see Fig. 8(c), corresponding to point B in Fig. 10);
- (II) if the cycle RL^{k+1} is degenerate, $\lambda_{k+2} = a_L^{k+1} a_R = -1$, so that $d_{k+1} = \mu_L$, then

$T_1(0) = \mu_L$, $T_1(\mu_L) = 0$ and by Property 3 the parameter point is $P_k \in \xi_{RL^k}^r \cap \theta_{RL^{k+1}} \cap C_N \cap \xi_{RL^{k+2}}^l$. F_R is continuous and invertible being the diagonal with slope -1 in the whole interval J_R , thus also f is invertible, all the points in J_R are cycles of period $2(k+2)$ except for the fixed point (the graph of F_R in the point P_k is shown in Fig. 10);

- (III) if the cycle RL^{k+1} is unstable then $T_1(\mu_L) < 0$, which also means that the discontinuity point $d_{k+1} = \mu_L / (|\lambda_{k+2}|) < \mu_L$ is inside the interval J_R and the first return map is defined by $T_1(x)$ for $0 < x < d_{k+1}$ with range $T_1([0, d_{k+1}]) = [\mu_L, 0]$ and by $T_2(x)$ for $d_{k+1} < x < \mu_L$, which means that in the definition in (35) the integer k is increased by 1, but also that the return map F_R (and thus f) is noninvertible (Fig. 9(c), corresponding to point C in Fig. 10).

For $a_L > 1$ and decreasing a_R , $-1 < a_R < 0$, we know that the flip bifurcation of the cycle RL^{k+1} of higher period occurs first, and at the bifurcation value, when $\lambda_{k+2} = a_L^{k+1} a_R = -1$, we have $T_1(\mu_L) = a_L^{k+1} a_R \mu_L - a_L^{k+1} a_R d_k + \mu_L = d_k$ (as in fact the first return map $T_1(x)$ has slope -1), and the cycle RL^k is still stable, in fact $0 > \lambda_{k+1} = a_L^k a_R > -1$ and $T_0(0) = a_L^k (\mu_R + \mu_L \phi_k^L) = (d_k/a_L) < d_k$, then the map F_R (and thus f) is invertible. To summarize, we have proved the following.

Theorem 3. Consider $a_L > 1$, $-1 < a_R < 0$ and the region of invertibility of f (below the set C_N). Then the return map F_R is either continuous in J_R (region (b) in Fig. 10), in which case there exists

a unique globally attracting cycle, or there exist at most one discontinuity point (regions (a) and (c) in Fig. 10), and thus with two cycles, one of which is necessarily stable.

- (i) In the overlapping region below the flip bifurcation curves (region (a) in Fig. 10), two stable cycles with symbol sequence RL^k and RL^{k+1} coexist, and no unstable cycle can exist. The points of the interval $(0, d_k)$ converge to the cycle with symbol sequence RL^k while the points of the interval (d_k, μ_L) converge to RL^{k+1} .
- (ii) In the region between two flip bifurcation curves there exists a unique stable cycle (region (c) in Fig. 10), attracting all the points except those of the coexistent unstable cycle.

Figure 10 illustrates the qualitative shape of the first return map F_R and related properties of the map f close to each of the infinitely many points P_k with $k > 1$ as shown in Fig. 7.

Notice that crossing through the particular points P_k , we can have a direct transition from regular regime to chaos, and thus infinitely many BCB curves must necessarily issue from such points.

While for $a_L < 1$ and decreasing a_R , s we know that the flip bifurcation of the cycle RL^k of lower period occurs first, however, as already remarked, only cycles of low periods (2, 3, 4) can be attracting. We shall see two examples in the following subsection.

5.4. Examples

As illustrative examples we show two bifurcation diagrams of increasing a_L , fixing $-1 < a_R < 0$

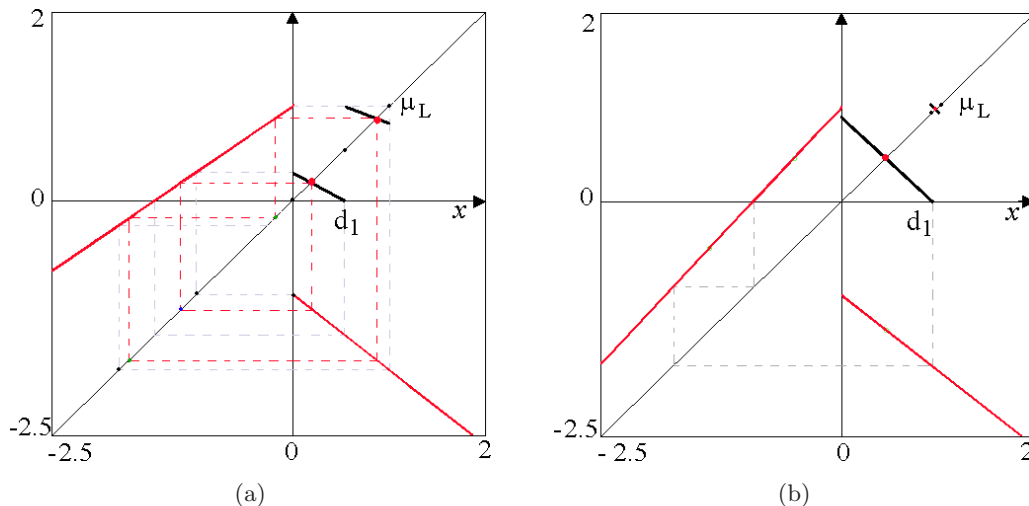


Fig. 11. Graph of the function f and first return map F_R at $\mu_R = -1$, $\mu_L = 1$ and $a_R = -0.8$. (a) $a_L = 0.7$. (b) $a_L = 1.09$.

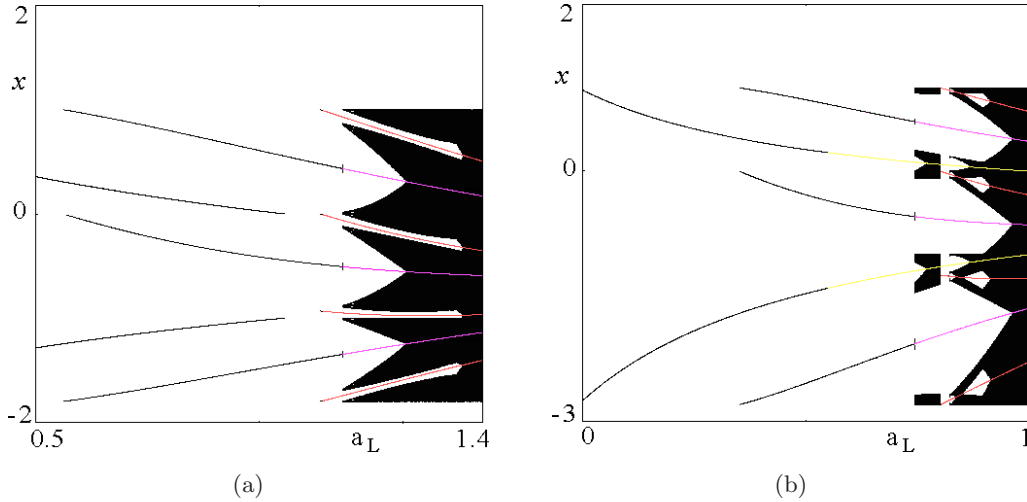


Fig. 12. One-dimensional bifurcation diagrams at $\mu_R = -1$ and $\mu_L = 1$, as a function of a_L . (a) $a_R = -0.8$. (b) $a_R = -1.8$.

and $a_R < -1$. Let us consider first the example in which $a_R = -0.8$ and we increase the parameter a_L from zero [Figs. 11 and 12(a)]. From the two-dimensional bifurcation diagram in Fig. 7 we know that we start with a stable 2-cycle, which is the only existing attractor as long as we cross the bifurcation curve $\xi_{RL^2}^l$ and an attracting 3-cycles coexists: in the first return map we have a discontinuity point d_1 [Fig. 11(a)].

The one-dimensional bifurcation diagram as a_L increases is shown in Fig. 12(a). The 2-cycle coexists with the 3-cycle up to the disappearance of the 2-cycle via BCB, crossing the BCB curve ξ_{RL}^l ($a_L\mu_R + \mu_L = 0$), leaving a unique 3-cycle up to the appearance of the 4-cycle as a_L crosses the BCB curve $\xi_{RL^3}^l$ (at $a_L = 1.0732$). In Fig. 12(a), we can see that the flip bifurcation of the 4-cycle

(at $a_L = 1.0772$) occurs before that of the 3-cycle (at $a_L = 1.118$), after which we only have chaotic dynamics. The first return map F_R in J_R when the 4-cycle is unstable and all the other points in I converge to the stable 3-cycle is shown in Fig. 11(b), where F_R is given by $T_0 = f_L^2 \circ f_R$ in $(0, d_1)$ and by $T_1 = f_L^3 \circ f_R$ in (d_1, μ_L) . The map becomes noninvertible when the 3-cycle is still stable, and at the flip-bifurcation of the 3-cycle, the dynamics become chaotic. When $T_1(\mu_L) = 0$ a new BCB curve $\xi_{RL^4}^r$ is crossed and a new discontinuity point d_2 appears in the first return map which is so defined:

$$\begin{aligned} T_0 &= f_L^2 \circ f_R && \text{in } (0, d_1), \\ T_1 &= f_L^3 \circ f_R && \text{in } (d_1, d_2), \\ T_2 &= f_L^4 \circ f_R && \text{in } (d_2, \mu_L) \end{aligned}$$

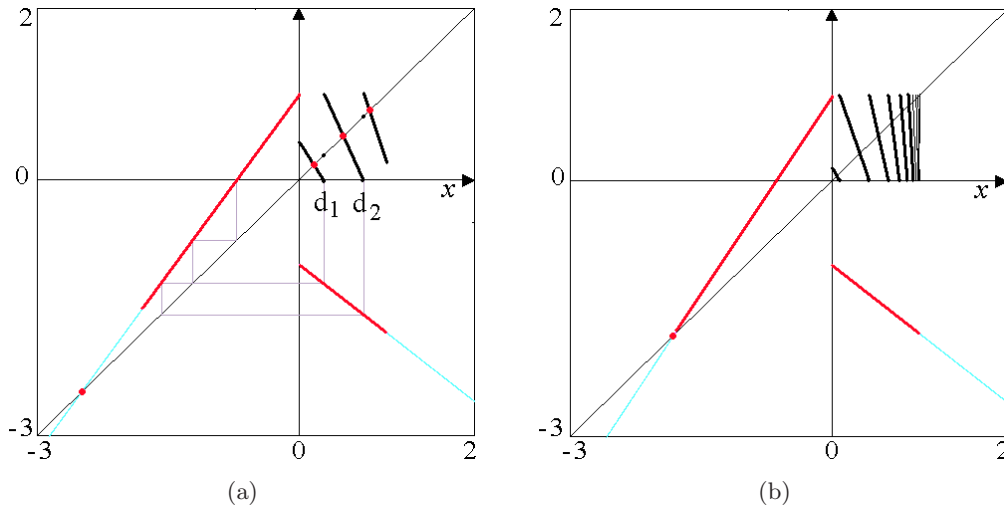


Fig. 13. Graph of the function f and first return map F_R at $\mu_R = -1$, $\mu_L = 1$ and $a_R = -0.8$. (a) $a_L = 1.4$. (b) $a_L = 1.55$.

as shown in Fig. 13(a). When $T_2(\mu_L) = 0$, a new BCB curve ξ_{RL}^L is crossed and a new discontinuity point d_3 appears and the first return map increases by one piece, by $T_3 = f_L^A \circ f_R$ in (d_3, μ_L) , and so on. The number of discontinuity points d_j and pieces in the return map tends to infinity as the final contact bifurcation with the unstable fixed point P^* is approached [see Fig. 13(b)]. The integer associated with the first discontinuity point increases by 1 whenever a periodicity region ceases to exist (as we increase the parameter a_L). In Fig. 12(b), we also show a one-dimensional bifurcation diagram at $a_R = -1.8$ and we increase the parameter a_L from 0. We can see that now the flip bifurcation of the 2-cycle occurs first, followed by the flip bifurcation of the 3-cycle and the last one is that of the 4-cycle.

References

- Avrutin, V. & Schanz, M. [2005] "Period-doubling scenario without flip bifurcations in a one-dimensional map," *Int. J. Bifurcation and Chaos* **15**, 1267–1284.
- Avrutin, V. & Schanz, M. [2006] "On multi-parametric bifurcations in a scalar piecewise-linear map," *Nonlinearity* **19**, 531–552.
- Avrutin, V., Schanz, M. & Banerjee, S. [2006] "Multi-parametric bifurcations in a piecewise-linear discontinuous map," *Nonlinearity* **19**, 1875–1906.
- Avrutin, V., Eckstein, B. & Schanz, M. [2007] "On detection of multiband chaotic attractors," *Proc. Roy. Soc. A* **463**, 1339–1358.
- Avrutin, V. & Schanz, M. [2008] "On the fully developed bandcount adding scenario," *Nonlinearity* **21**, 1077–1103.
- Avrutin, V., Eckstein, B. & Schanz, M. [2008a] "The bandcount increment scenario. I. Basic structures," *Proc. Roy. Soc. A* **464**, 1867–1883.
- Avrutin, V., Eckstein, B. & Schanz, M. [2008b] "The bandcount increment scenario. II. Interior structures," *Proc. Roy. Soc. A* **464**, 2247–2263.
- Avrutin, V., Eckstein, B. & Schanz, M. [2009] "The bandcount increment scenario. III. Deformed structures," *Proc. Roy. Soc. A* **465**, 41–57.
- Avrutin, V., Schanz, M. & Gardini, L. [2010a] "On a special type of border-collision bifurcations occurring at infinity," *Physica D* **239**, 1083–1094.
- Avrutin, V., Schanz, M. & Gardini, L. [2010b] "Computation of bifurcation curves by map replacement," *Int. J. Bifurcation and Chaos* **20**.
- Avrutin, V., Schanz, M. & Gardini, L. [2010c] "Self-similarity of the bandcount adding: Calculation by map replacement," *Regul. Chaot. Dyn.* **15**, 683–701.
- Banerjee, S., Yorke, J. A. & Grebogi, C. [1998] "Robust chaos," *Phys. Rev. Lett.* **80**, 3049–3052.
- Banerjee, S. & Grebogi, C. [1999] "Border-collision bifurcations in two-dimensional piecewise smooth maps," *Phys. Rev. E* **59**, 4052–4061.
- Banerjee, S., Karthik, M. S., Yuan, G. H. & Yorke, J. A. [2000] "Bifurcations in one-dimensional piecewise smooth maps — theory and applications in switching circuits," *IEEE Trans. Circ. Syst.-I* **47**, 389–394.
- Banerjee, S. & Verghese, G. C. (eds.) [2001] *Nonlinear Phenomena in Power Electronics: Attractors, Bifurcations, Chaos, and Nonlinear Control* (IEEE Press, NY).
- di Bernardo, M., Feigin, M. I., Hogan, S. J. & Homer, M. E. [1999] "Local analysis of C-bifurcations in n-dimensional piecewise smooth dynamical systems," *Chaos Solit. Fract.* **10**, 1881–1908.
- di Bernardo, M., Budd, C. J., Champneys, A. R. & Kowalczyk, P. [2008] *Piecewise-Smooth Dynamical Systems, Theory and Applications* (Springer Verlag, NY).
- Gardini, L., Tramontana, F., Avrutin, V. & Schanz, M. [2010] "Border collision bifurcations in 1D PWL map and the Leonov approach," submitted for publication.
- Halse, C., Homer, M. & di Bernardo, M. [2003] "C-bifurcations and period-adding in one-dimensional piecewise-smooth maps," *Chaos Solit. Fract.* **18**, 953–976.
- Ing, J., Pavlovskaja, E., Wiercigroch, M. & Banerjee, S. [2008] "Experimental study of impact oscillator with one-sided elastic constraint," *Phil. Trans. Royal Soc. A* **366**, 679–704.
- Kollar, L. E., Stepan, G. & Turi, J. [2004] "Dynamics of piecewise-linear discontinuous maps," *Int. J. Bifurcation and Chaos* **14**, 2341–2351.
- Leonov, N. N. [1959] "Map of the line onto itself," *Radiofizika* **3**, 942–956.
- Leonov, N. N. [1962] "Discontinuous map of the straight line," *Dokl. Acad. Nauk SSSR* **143**, 1038–1041.
- Maistrenko, Y. L., Maistrenko, V. L. & Chua, L. O. [1993] "Cycles of chaotic intervals in a time-delayed Chua's circuit," *Int. J. Bifurcation and Chaos* **3**, 1557–1572.
- Maistrenko, Y. L., Maistrenko, V. L., Vikul, S. I. & Chua, L. O. [1995] "Bifurcations of attracting cycles from time-delayed Chua's circuit," *Int. J. Bifurcation and Chaos* **5**, 653–671.
- Maistrenko, Y. L., Maistrenko, V. L. & Vikul, S. I. [1998] "On period-adding sequences of attracting cycles in piecewise linear maps," *Chaos Solit. Fract.* **9**, 67–75.
- Mira, C. [1978] "Sur les structure des bifurcations des difféomorphisme du cercle," *C. R. Acad. Sc. Paris, Series A* **287**, 883–886.
- Mira, C. [1987] *Chaotic Dynamics* (World Scientific, Singapore).

- Nusse, H. E. & Yorke, J. A. [1992] “Border-collision bifurcations including period two to period three for piecewise smooth systems,” *Physica D* **57**, 39–57.
- Nusse, H. E., Ott, E. & Yorke, J. A. [1994] “Border-collision bifurcations: An explanation for observed bifurcation phenomena,” *Phys. Rev. E* **49**, 1073–1076.
- Nusse, H. E. & Yorke, J. A. [1995] “Border-collision bifurcations for piecewise smooth one-dimensional maps,” *Int. J. Bifurcation and Chaos* **5**, 189–207.
- Pavlovskaja, E., Wiercigroch, M. & Grebogi, C. [2004] “Two-dimensional map for impact oscillator with drift,” *Phys. Rev. E* **70**, 036201.
- Pavlovskaja, E. & Wiercigroch, M. [2007] “Low-dimensional maps for piecewise smooth oscillators,” *J. Sound Vibr.* **305**, 750–771.
- Sharan, R. & Banerjee, S. [2008] “Character of the map for switched dynamical systems for observations on the switching manifold,” *Phys. Lett. A* **372**, 4234–4240.
- Sushko, I., Agliari, A. & Gardini, L. [2005] “Bistability and border-collision bifurcations for a family of unimodal piecewise smooth maps,” *Discr. Contin. Dyn. Syst. Series B* **5**, 881–897.
- Sushko, I., Agliari, A. & Gardini, L. [2006] “Bifurcation structure of parameter plane for a family of unimodal piecewise smooth maps: Border-collision bifurcation curves,” *Chaos Solit. Fract.* **29**, 756–770.
- Sushko, I. & Gardini, L. [2010] “Degenerate bifurcations and border collisions in piecewise smooth 1D and 2D maps,” *Int. J. Bifurcation and Chaos* **20**, 2045–2070.
- Zhusubaliyev, Z. T. & Mosekilde, E. [2003] *Bifurcations and Chaos in Piecewise-Smooth Dynamical Systems* (World Scientific, Singapore).